Supplement of Biogeosciences, 18, 6547–6565, 2021
https://doi.org/10.5194/bg-18-6547-2021-supplement

Biogeosciences
Open Access

Supplement of

Evaluation of carbonyl sulfide biosphere exchange in the Simple Biosphere Model (SiB4)

Linda M. J. Kooijmans et al.

Correspondence to: Linda M. J. Kooijmans (linda.kooijmans@wur.nl)

Supplementary information for **Evaluation of carbonyl sulfide biosphere exchange in the Simple Biosphere Model (SiB4)**

Linda M.J. Kooijmans et al.

Correspondence to: Linda Kooijmans (linda.kooijmans@wur.nl)

Table S1. Site information of long-term CO_2 flux measurements from FLUXNET, AmeriFlux or ICOS, including mean annual temperature (MAT) and mean annual precipitation (mm).

	Network	Lat (°N), Lon (°E)	Years	MAT (°C)	MAP (mm)	Reference
Hyytiälä, Finland (FI-HYY)	ICOS	61.8, 24.3	1996-2018	3.8	709	Kolari et al. (2009)
Sorø, Denmark (DK-SOR)	ICOS	55.5, 11.6	1996-2018	8.2	660	Pilegaard et al. (2011); Wu et al. (2013).
Neustift, Austria (AT-NEU)	FLUXNET-2015	47.1, 11.3	2002-2012	6.5	852	Wohlfahrt et al. (2008) DOI:10.18140/FLX/1440121
Harvard Forest, US (US-HA1)	FLUXNET-2015	42.5, -72.2	1991-2012	6.6	1071	DOI:10.18140/FLX/1440071
Fermilab, US (US-IB2)	FLUXNET-2015	41.8, -88.2	2004-2011	9.0	930	Matamala et al. (2008) DOI:10.17190/AMF/1246066
Bondville, US (US-BO1)	AMERI-FLUX	40.0, -88.3	1996-2008	11.0	991	DOI:10.17190/AMF/1246036
Majadas, Spain (ES-LM1)	ICOS	39.9, -5.8	2014-2018	16.0	700	El-Madany et al. (2018)
ARM Southern Great Plains, US (US-ARM)	FLUXNET-2015	36.6, -97.5	2003-2012	14.8	843	DOI:10.18140/FLX/1440066

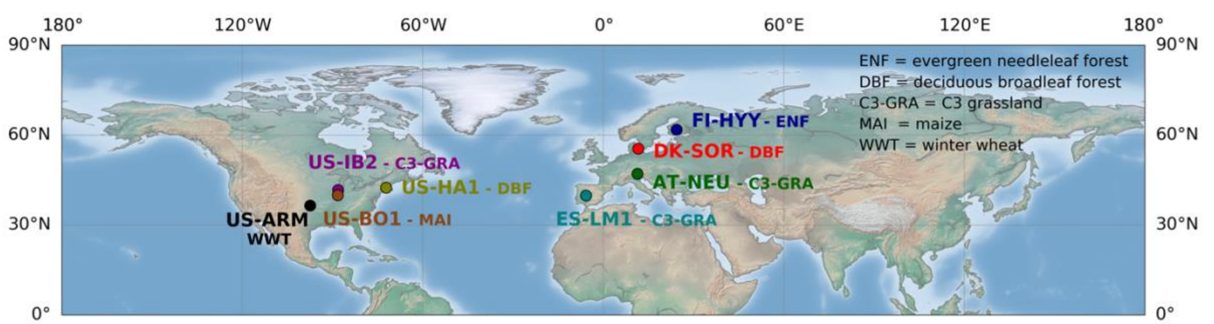

Figure S1. Location of measurement sites and information on the PFT they represent.

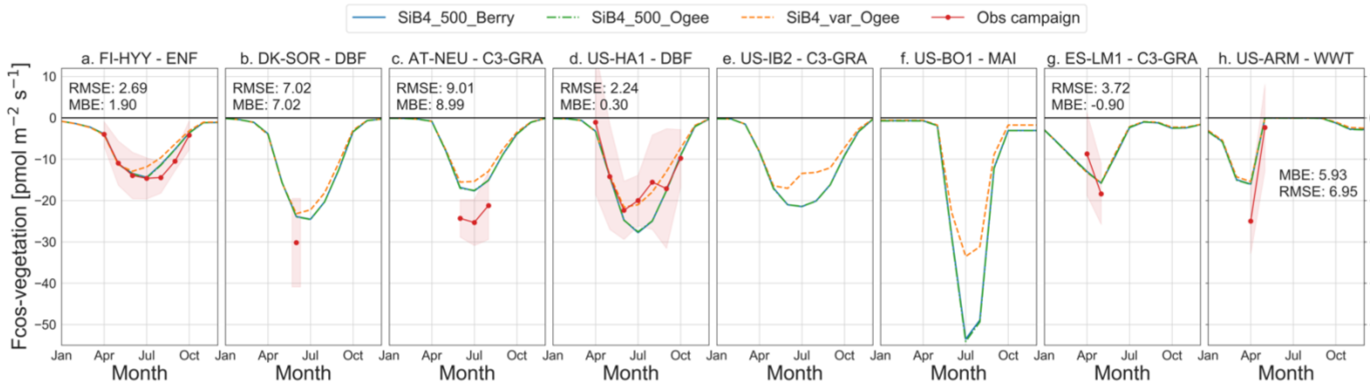

Figure S2. Comparison of COS vegetation flux seasonal cycles of observations (red) with different SiB4 model runs: SiB4_500_Berry (blue, solid), SiB4_var_Ogee (orange, dashed), SiB4_500_Ogee (green, dot-dash). Monthly averages are shown with the 1σ spread around the mean of observations. Negative values indicate uptake of COS by the ecosystem while positive values indicate COS emissions. The model simulations are from the same year(s) in which observations were made. The MBE and RMSE (pmol m^{-2} s^{-1}) are given for monthly average fluxes. Sites are presented from high to low latitude.

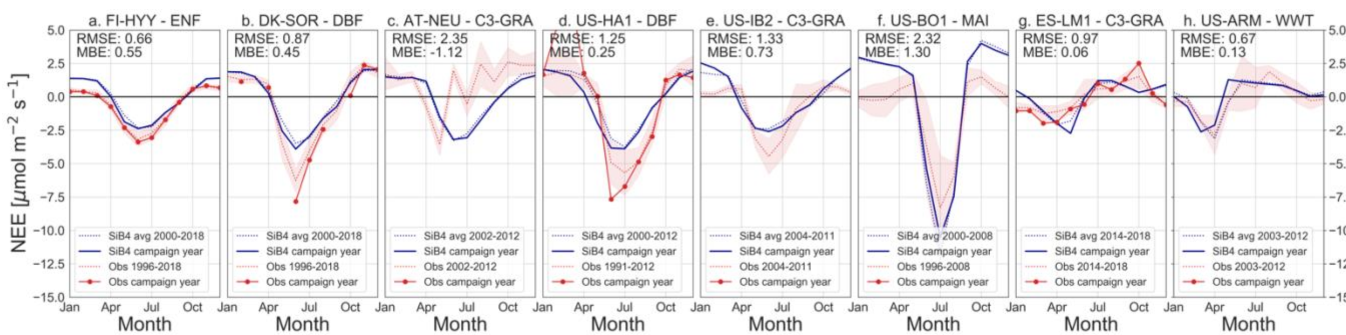

Figure S3. Comparison of NEE seasonal cycles of SiB4 model simulations (blue) with observations from either FLUXNET, AmeriFlux or ICOS (indicated in legend) (red). Monthly averages are shown with the 1σ spread around the mean of observations. Negative values indicate uptake of CO_2 by the ecosystem while positive values indicate CO_2 emissions. The model simulations represent the years in which observations were made from 2000 onwards. The MBE and RMSE (μmol m^{-2} s^{-1}) are given for monthly average fluxes.

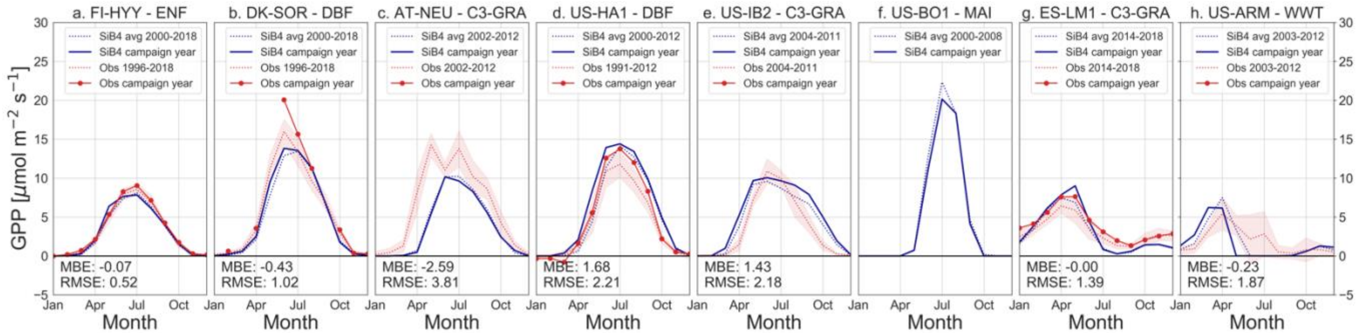

Figure S4. Comparison of GPP seasonal cycles of SiB4 model simulations (blue) with observations from either FLUXNET, AmeriFlux or ICOS (indicated in legend) (red). Monthly averages are shown with the 1σ spread around the mean of observations. The model simulations represent the years in which observations were made from 2000 onwards. The MBE and RMSE (μmol m^{-2} s^{-1}) are given for monthly average fluxes.

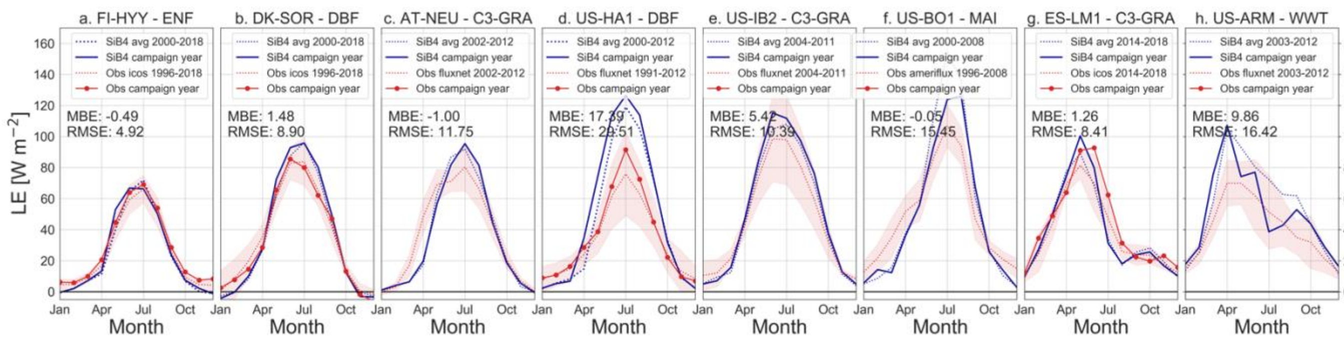

Figure S5. Comparison of LE seasonal cycles of SiB4 model simulations (blue) with observations from either FLUXNET, AmeriFlux or ICOS (indicated in legend) (red). The model simulations represent the years in which observations were made from 2000 onwards. The MBE and RMSE (W m^{-2}) are given for monthly average fluxes.

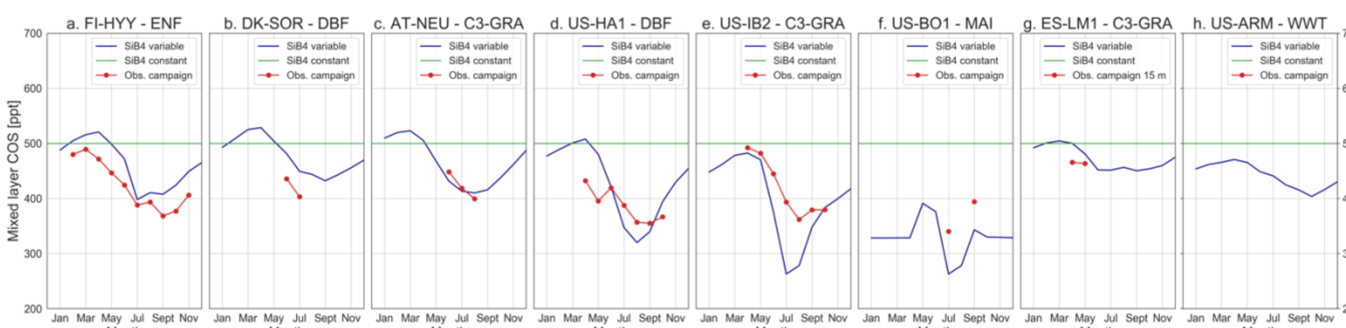

Figure S6: Seasonal cycles of COS mole fractions as used in the SiB4 simulations (blue and green) together with observed COS mole fractions above or in the canopy. No COS mole fraction observations are available for US-ARM.

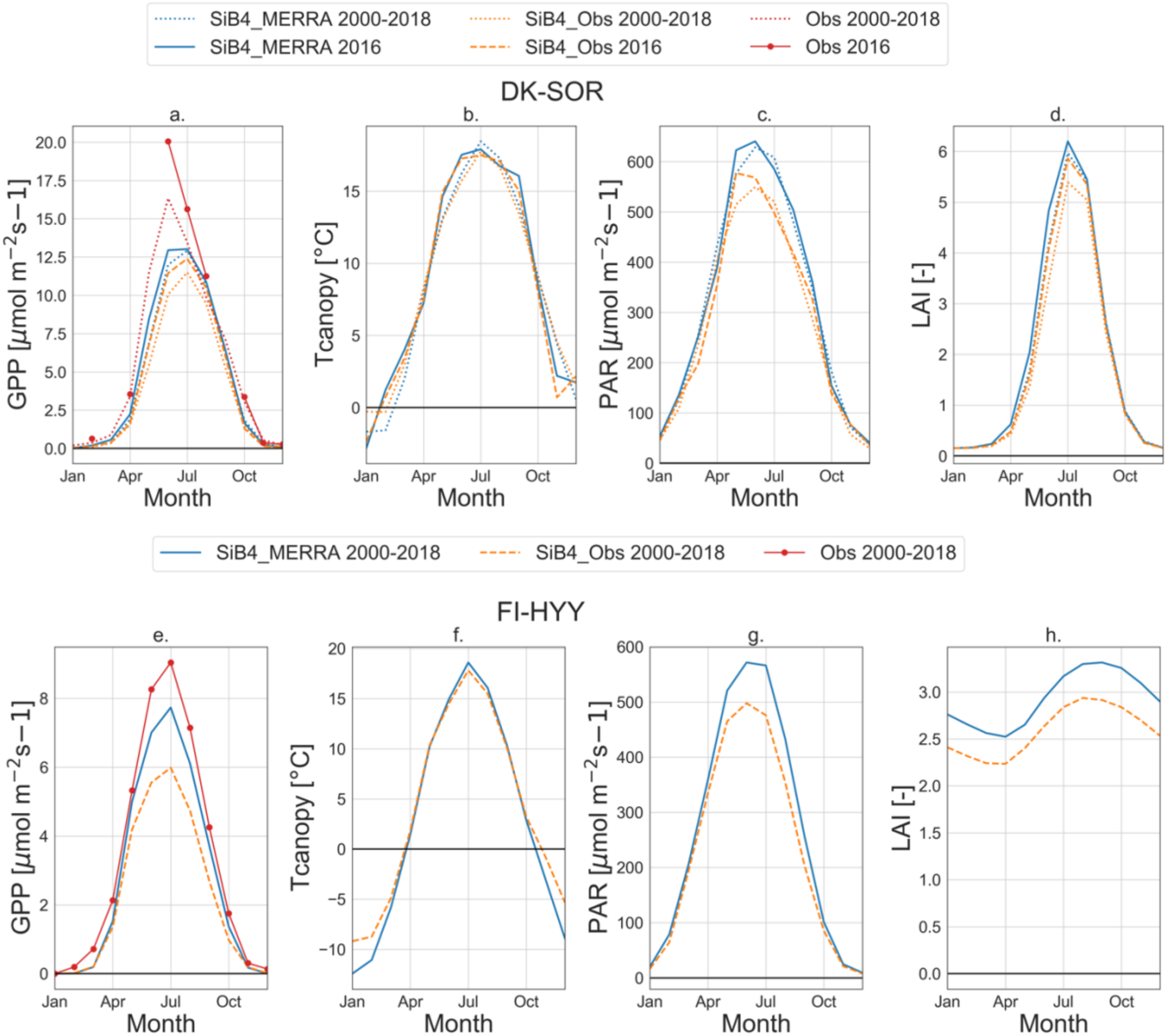

Figure S7: Seasonal cycles of GPP, canopy temperature (Tcanopy), photosynthetically active radiation (PAR) and leaf area index (LAI) at DK-SOR (top) and FI-HYY (bottom) as simulated by SiB4 with MERRA2 driver data (blue) and as simulated by SiB4 with observed site meteorology (orange) and compared with GPP observations from ICOS.

Simulated GPP is consistently lower in SiB4_Obs due to lower radiation in the observations than in MERRA2 (Fig. S7c,g), leading to a larger GPP model-observation bias with SiB4_Obs (Fig. S7a,e). A reason for the larger bias when site meteorology is used is that all of the tests, development and tuning for SiB4 are done with MERRA2 driver files, which might be different for site-level meteorological input. The results in the main text are consistently based on SiB4 runs with MERRA2 driver data, and are not biased by using different meteorology than in the SiB4 development.

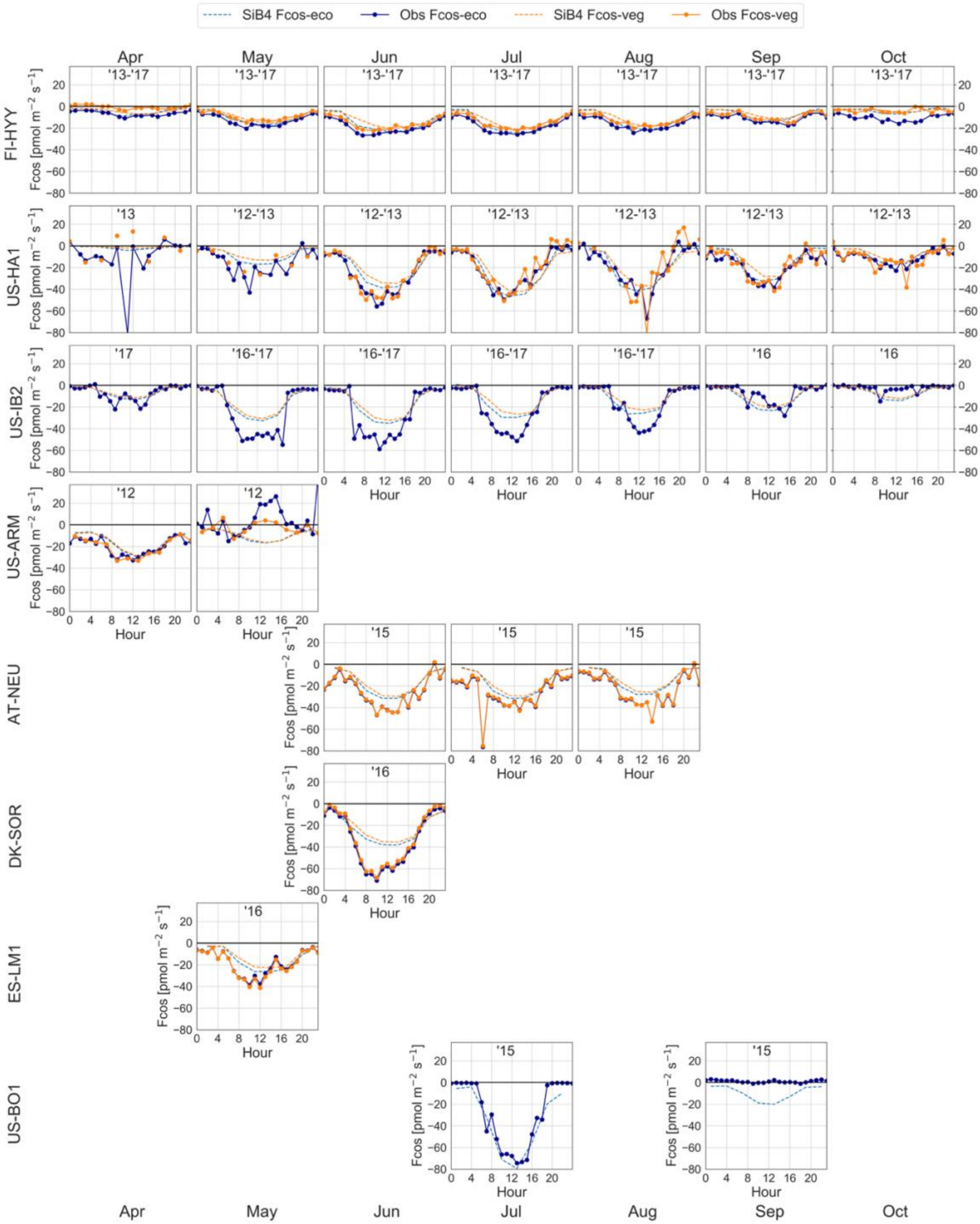

Figure S8. Diurnal cycles of COS ecosystem (blue) and vegetation (orange) fluxes as observed (dotted line) and simulated (dashed line) per month and per site. Model results represent settings from SiB4_var_Ogee. Negative values indicate uptake of COS by the ecosystem while positive values indicate COS emissions.

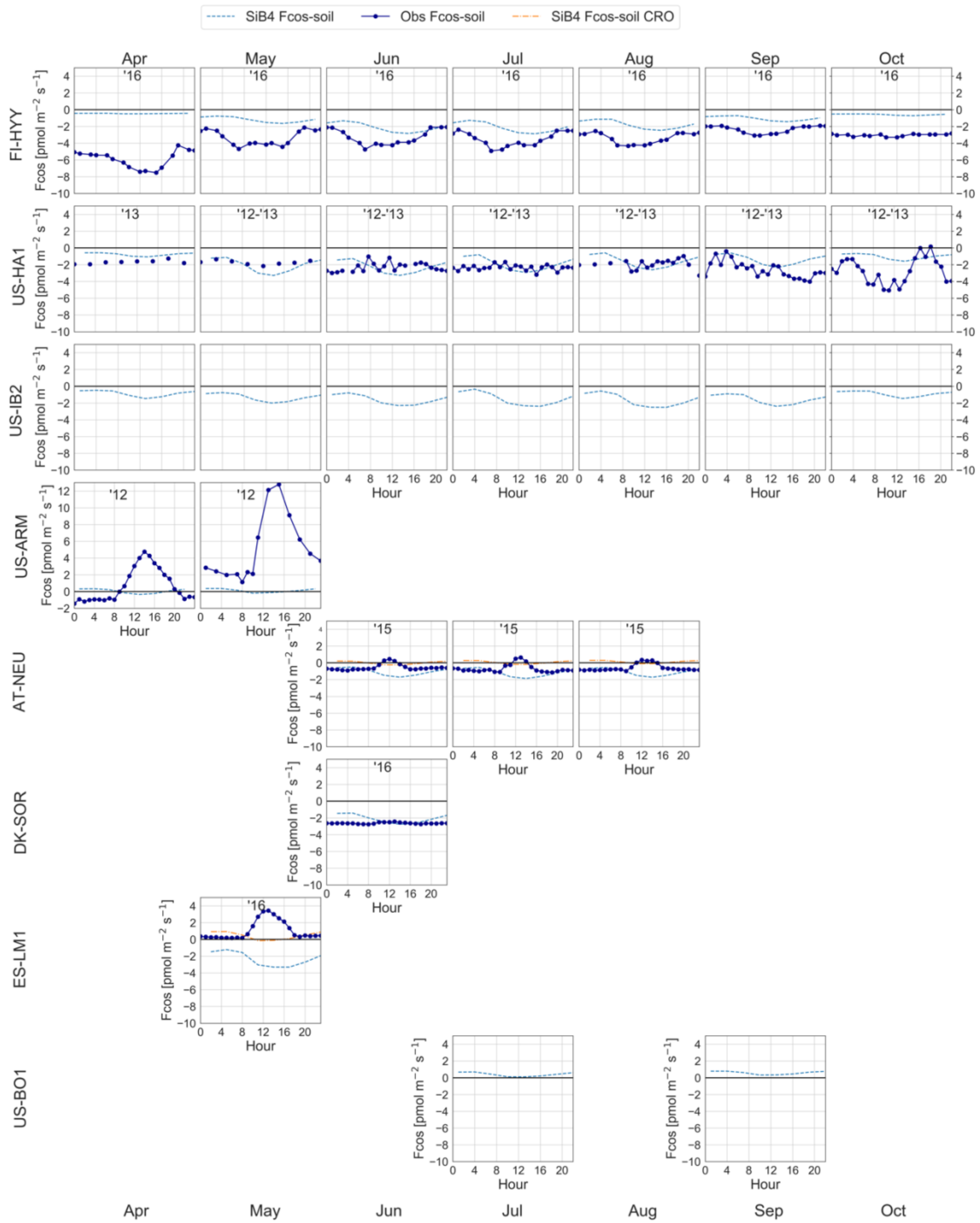

Figure S9. Diurnal cycles of COS *soil* fluxes as observed (dotted line) and simulated (dashed line) per month and per site. Model results represent settings from SiB4_var_Ogee with the simulation representing the biome (soil) type as indicated in Table 3 of the main text. For AT-NEU and ES-LM1 an extra simulation representing agricultural soil is shown. Positive fluxes represent uptake by the soil. Negative values indicate uptake of COS by the ecosystem while positive values indicate COS emissions.

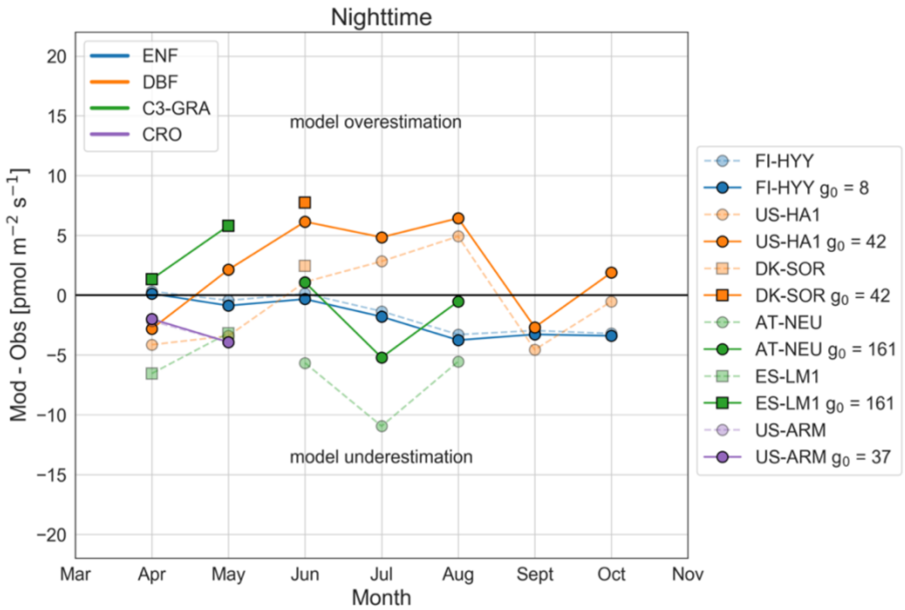

Figure S10. Difference between model simulations and observations of monthly average COS vegetation fluxes (ecosystem – soil) for nighttime data (21 – 03 hr) based on two different minimum stomatal conductance settings. The runs with original SiB4 minimum stomatal conductance values (10 mmol m^{-2} s^{-1} for most PFTs, and 40 mmol m^{-2} s^{-1} for C4 plants and crops) are shown as transparent dashed lines (equal to those shown in Fig. 3 of the main text). The runs with modified minimum stomatal conductance as adopted by Lombardozzi et al. (2017) (values indicated in the legend, unit in mmol m^{-2} s^{-1}, see also Table S2) are shown as solid lines. All runs are done with settings following SiB4_var_Ogee.

Table S2. Minimum stomatal conductance (g_0) values used as default in SiB4 and those adopted from Lombardozzi et al. (2017). Units are in mmol m^{-2} s^{-1}.

PFT	Sites	Default SiB4 g_0	Adjusted g_0
ENF	FI-HYY	10	8
DBF	US-HA1, DK-SOR	10	42
C3-GRA	AT-NEU, ES-LM1	10	161
WWT	US-ARM	40	37

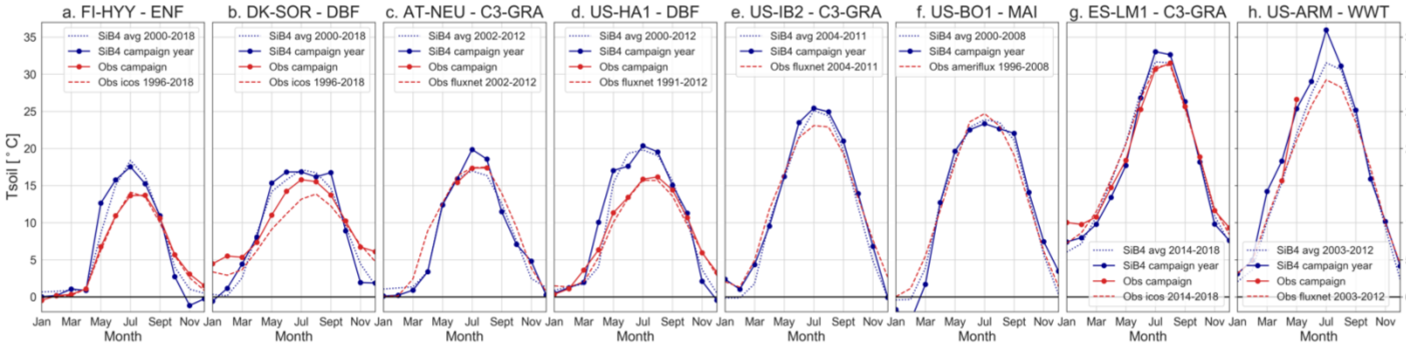

Figure S11. Comparison of soil temperature seasonal cycles as measured by the FLUXNET, AmeriFlux or ICOS network at 0.05 m (red) and simulated in the upper two soil layers (0-0.13 m by the SiB4 model (blue). The model simulations are from the same year(s) in which observations were made.

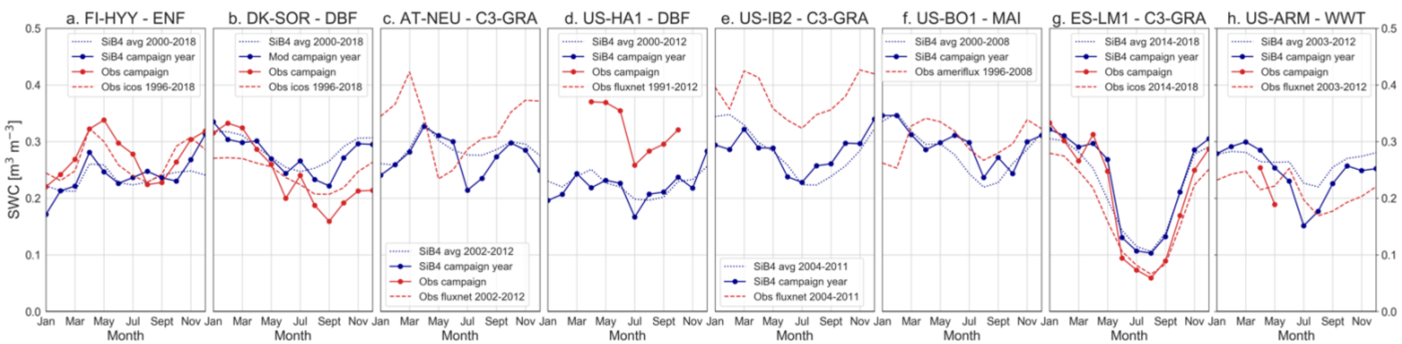

Figure S12. Comparison of soil moisture as measured by the FLUXNET, AmeriFlux or ICOS network at 0.05 m (red) and simulated in the upper two soil layers (0-0.13 m) by the SiB4 model (blue). The model simulations are from the same year(s) in which observations were made.

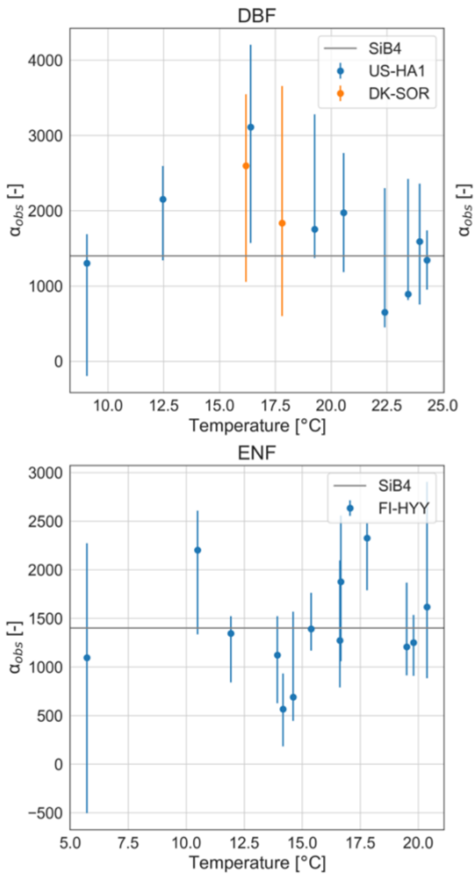

Figure S13. Correlation of α_{obs} against air temperature based on two-weekly medians, separated by PFT. Error bars represent the 25^{th}-75^{th} percentiles.

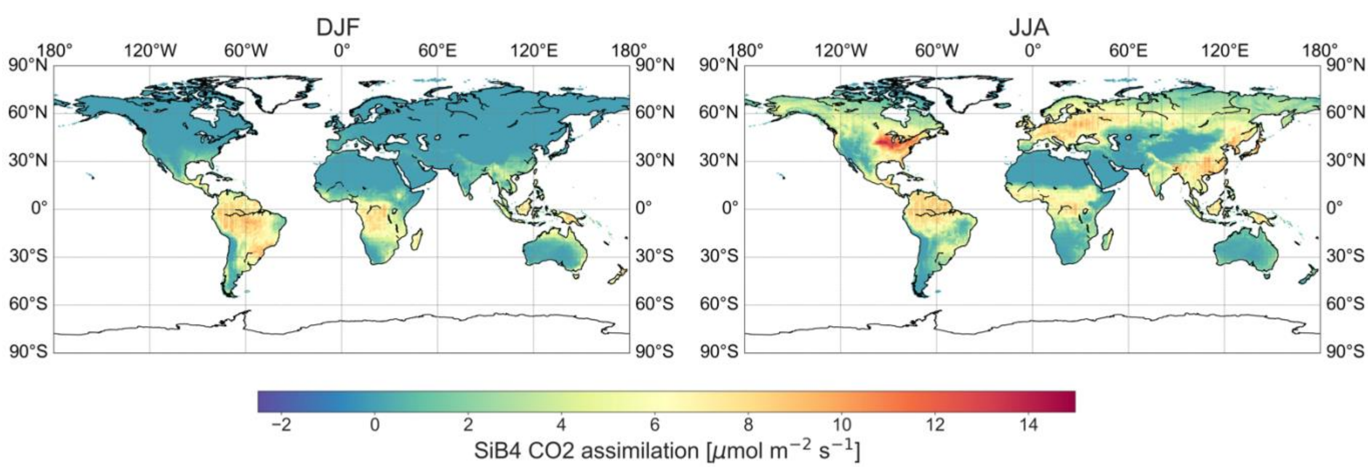

Figure S14. Global distribution of CO_2 assimilation in DJF (left) and JJA (right) as simulated by SiB4_var_Ogee over the years 2000-2020. Positive values (red) indicate CO_2 uptake by the biosphere.

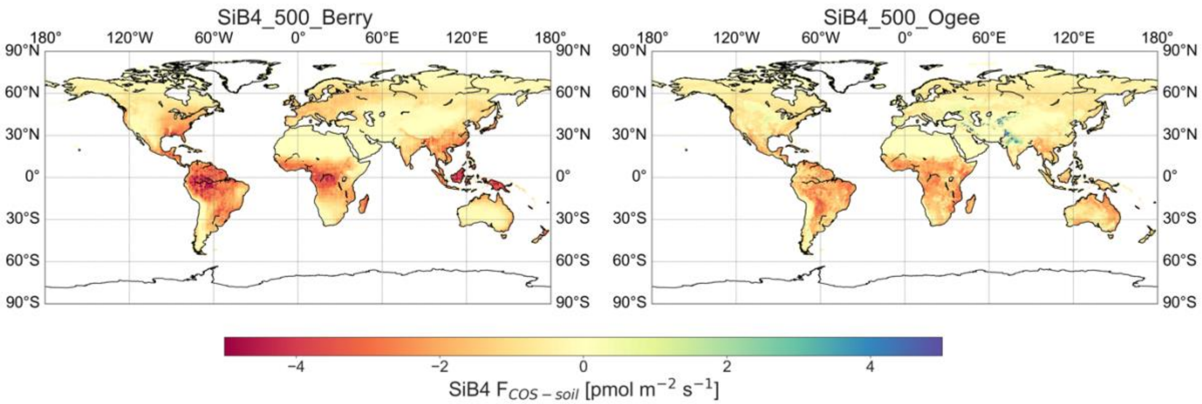

Figure S15. Global distribution of the COS soil flux as simulated by SiB4_500_Berry (left) and SiB4_500_Ogee. Negative values indicate uptake of COS by the biosphere while positive values indicate COS emissions.

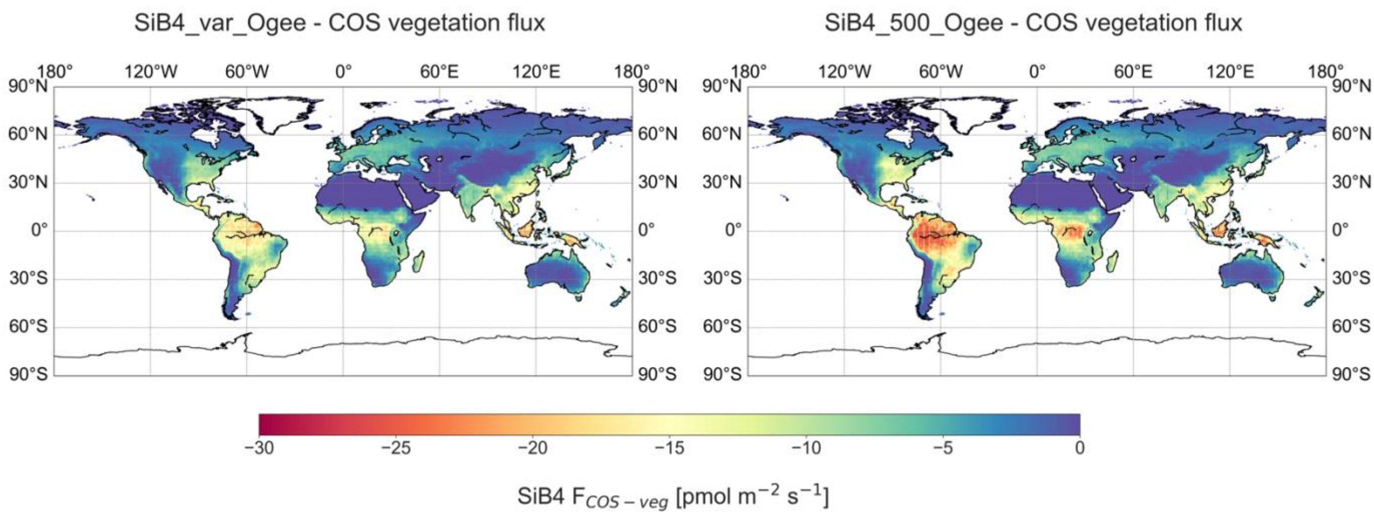

Figure S16. Global distribution of the COS vegetation flux as simulated by SiB4_var_Ogee (left) and SiB4_500_Ogee (right). Negative values indicate uptake of COS by the biosphere while positive values indicate COS emissions.

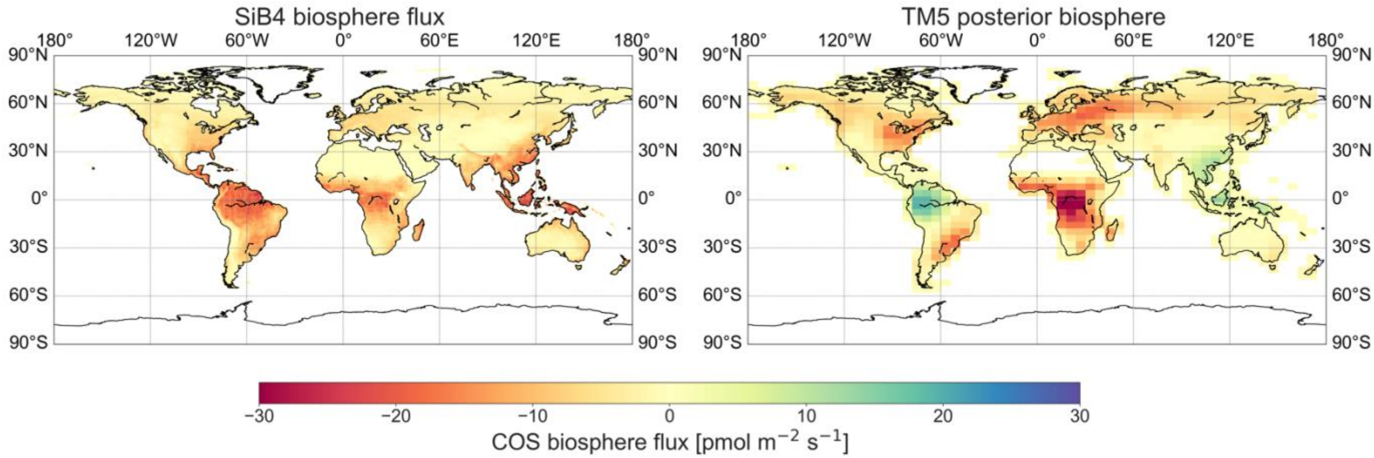

Figure S17. Global distribution of the COS vegetation flux as simulated by SiB4_var_Ogee (left) and the posterior biosphere flux as presented by Ma et al. (2021).

References in supplementary information

El-Madany, T. S., Reichstein, M., Perez-Priego, O., Carrara, A., Moreno, G., Pilar Martín, M., Pacheco-Labrador, J., Wohlfahrt, G., Nieto, H., Weber, U., Kolle, O., Luo, Y.-P., Carvalhais, N. and Migliavacca, M.: Drivers of spatio-temporal variability of carbon dioxide and energy fluxes in a Mediterranean savanna ecosystem, Agric. For. Meteorol., 262, 258–278, doi:https://doi.org/10.1016/j.agrformet.2018.07.010, 2018.

Kolari, P., Kulmala, L., Pumpanen, J., Launiainen, S., Ilvesniemi, H., Hari, P. and Nikinmaa, E.: CO2 exchange and component CO2 fluxes of a boreal Scots pine forest, Boreal Environ. Res., 14, 761–783, 2009.

Lombardozzi, D. L., Zeppel, M. J. B., Fisher, R. A. and Tawfik, A.: Representing nighttime and minimum conductance in CLM4.5: global hydrology and carbon sensitivity analysis using observational constraints, Geosci. Model Dev., 10(1), 321–331, doi:10.5194/gmd-10-321-2017, 2017.

Matamala, R., Jastrow, J. D., Miller, R. M. and Garten, C. T.: Temporal changes in C and N stocks of restored prairie: Implications for C sequestration strategeies, Ecol. Appl., 18(6), 1470–1488, doi:https://doi.org/10.1890/07-1609.1, 2008.

Pilegaard, K., Ibrom, A., Courtney, M. S., Hummelshøj, P. and Jensen, N. O.: Increasing net CO2 uptake by a Danish beech forest during the period from 1996 to 2009, Agric. For. Meteorol., 151(7), 934–946, doi:https://doi.org/10.1016/j.agrformet.2011.02.013, 2011.

Wohlfahrt, G., Hammerle, A., Haslwanter, A., Bahn, M., Tappeiner, U. and Cernusca, A.: Seasonal and inter-annual variability of the net ecosystem CO2 exchange of a temperate mountain grassland: Effects of weather and management, J. Geophys. Res. Atmos., 113(D8), doi:https://doi.org/10.1029/2007JD009286, 2008.

Wu, J., Larsen, K. S., van der Linden, L., Beier, C., Pilegaard, K. and Ibrom, A.: Synthesis on the carbon budget and cycling in a Danish, temperate deciduous forest, Agric. For. Meteorol., 181, 94–107, doi:https://doi.org/10.1016/j.agrformet.2013.07.012, 2013.